Cyclotron resonance with 10^{-11} resolution: Anharmonic detection and beating a coherent drive with the noise

F. L. Moore, L. S. Brown, D. L. Farnham, S. Jeon, P. B. Schwinberg, and R. S. Van Dyck, Jr.
Department of Physics, FM-15, University of Washington, Seattle, Washington 98195
(Received 27 August 1991)

We describe the detection of the radial motions of a trapped charge in a Penning trap via a fourth-order electrostatic coupling to the axial degree of freedom. Two basic approaches are demonstrated. The first uses a standard resonant drive to determine the cyclotron frequency and has a resolution of 0.1 ppb. The second approach beats the motion due to an off-resonant drive against the motion due to thermal drives to give a continuous phase-coherent monitor of the cyclotron motion with a resolution of 0.01 ppb. The inherent systematic shift of these "anharmonic-detection" schemes is discussed, and approaches are given to reduce or eliminate it.

PACS number(s): 07.75.+h, 35.10.Bg, 29.90.+r, 41.70.+t

I. INTRODUCTION

The precision measurement of the cyclotron resonance of a charged particle in a Penning trap is crucial to the current measurements of the proton-electron mass ratio [1], several atomic and molecular masses [2–5], and the electron's magnetic moment [6,7]. It is also fundamental to tests of QED through comparisons of the electron's anomaly [8] a_e and tests of CPT invariance by looking for particle-antiparticle asymmetries in such comparisons as the g value of the positron to that of the electron [9] and the charge-to-mass ratios of both the positron to the electron [10] and the antiproton to the proton [11]. There are also proposals to test QED in the high-field limit by weighing the Lamb shift of hydrogenlike uranium [12] and to measure [13,14] the fine-structure constant, again via cyclotron measurements in a Penning trap.

This paper describes our current method of detecting the cyclotron frequency through observable shifts in the axial frequency when resonant cyclotron drives are applied. Our methods deviate from those of competing approaches [4–6] in that the coupling of the radial energy into the axial degree of freedom is through a weak fourth-order electrostatic term. In the first scheme the cyclotron drive is swept in frequency and a triggered, possibly nonequilibrium, axial shift occurs when the drive passes through resonance. A typical cyclotron resolution of about 0.1 ppb is experimentally observed. In addition, a method will be described that utilizes the beating of a coherent off-resonant cyclotron drive against the thermal cyclotron motion present at 4 K. In this method, equilibrium conditions are maintained in all degrees of freedom, enabling a continuous phase-sensitive monitor of the cyclotron motion. This may extend our cyclotron resolution to beyond 0.01 ppb. It should be noted that our current spectrometer has systematic cyclotron shifts, primarily due to magnetic field instabilities that enter just under the 1.0 ppb level; however, we now understand that the major instability is not from external sources of field variation, but from changes in susceptibility of materials passing through the high-field bore whose distribution varies as the external pressure varies. A solution to this problem (i.e., controlling pressure over the experiment) has been demonstrated [15] to yield long-term stability on the order of 0.2 ppb/h.

We assume that the reader is familiar with the basic oscillatory motions of a charged particle in a harmonic Penning trap and therefore give only physical justification for these motions. We refer the reader to Refs. [16,17] in the literature for a more detailed description. Figure 1 is a scaled drawing of the Penning trap used to take all the data presented in this article. It consists of five cylindrically symmetric electrodes designed to generate the quadratic electric potential

$$V = V_0 \frac{z^2 - \rho^2/2}{2d^2} . \tag{1.1}$$

Here V_0 is roughly the potential difference between the ring and end-cap electrodes, and d is the characteristic dimension of the trap,

$$d^2 = \frac{Z_0^2 + R_0^2/2}{2} , \tag{1.2}$$

where R_0 is the minimum ring radius and Z_0 is half the minimum end-cap spacing. The quadratic nature of this potential confines the motion of a charged particle along the z axis of cylindrical symmetry and induces harmonic motion at an angular frequency given by

$$\omega_z^2 = \frac{eV_0}{md^2} . \tag{1.3}$$

Radial confinement is provided by a 5-T magnetic field **B** applied along the z symmetry axis. This induces a cyclotronlike motion at the frequency

$$\omega_c' = \omega_c - \frac{\omega_z^2}{2\omega_c'} , \tag{1.4}$$

which is the free-space cyclotron motion at $\omega_c = eB/mc$

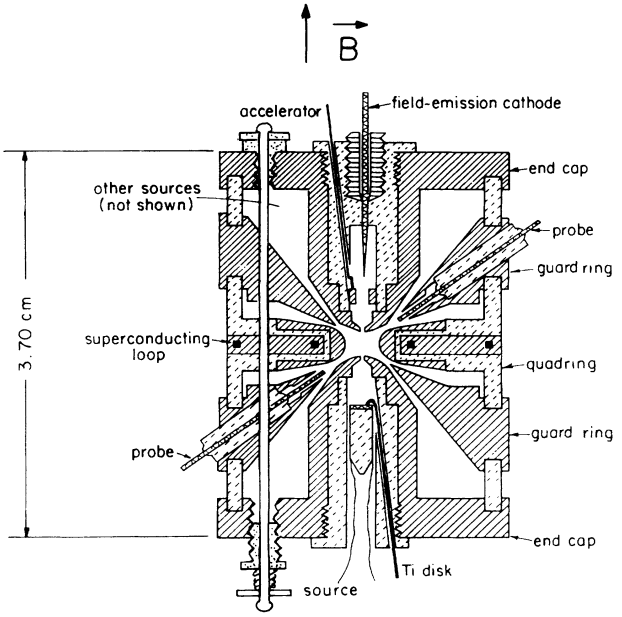

FIG. 1. Detailed scale drawing of actual Penning trap used. The hyperbolic end caps are at dc ground and the hyperbolic quadring is at potential V_0. This produces a harmonic electrostatic well in the axial direction. The potential on the guard electrodes is adjusted to minimize the fourth-order electrostatic terms of the trap. Radial confinement comes from the 5-T axial magnetic field which is stabilized by a superconducting double loop [18] placed in the quadring electrode. Also shown are the field-emission cathode, accelerator, and Ti reflection disk which generate a variable energy, multipass, ionizing electron beam. The probe electrodes are used to produce the necessary spatial gradient in the sideband cooling drive.

reduced by the perturbation caused by the radial electric field. This perturbation is the familiar $\mathbf{E}\times\mathbf{B}$ drift velocity which, coupled with the azimuthal symmetry of the trapping fields, generates a slow circular "magnetron" motion at the frequency

$$\omega_m = \frac{\omega_z^2}{2\omega_c'} \ . \tag{1.5}$$

Ideally, using Eqs. (1.4) and (1.5), the free-space cyclotron frequency can be obtained by measuring ω_c' and one of the other two normal-mode frequencies. (Using this procedure, we determine that ω_c will differ from the ideal value by no more than 1 ppb under typical operating conditions for which the measured and calculated ω_m differ by no more than 1 Hz.) Nevertheless, in practice it is more prudent to measure all three normal-mode frequencies and to derive the free-space cyclotron frequency by using the quadrature invariance theorem [19]

$$\omega_c^2 = (\omega_c')^2 + \omega_z^2 + \omega_m^2 \ , \tag{1.6}$$

which can be obtained by squaring Eq. (1.4). Equation (1.6) has been shown [19] to be invariant under all quadratic field perturbations such as cross terms due to an elliptical electric field geometry in addition to a misalignment between the magnetic field and the trap's electric axis of symmetry.

While it is possible to detect and measure all three normal modes directly via the currents they induce in the trap's electrodes [20], this is cumbersome because it requires several carefully tuned preamplifiers for each ion species to be studied in the trap. In addition, direct detection of the image currents of the cyclotron motion requires a strong coupling to the preamplifier. This strong coupling necessarily broadens the cyclotron resonance and can therefore reduce the resolution of this resonance. Similarly, the strong coupling to the preamplifier necessary to directly observe the magnetron motion would also adversely affect it. In this case, it would drive the ions radially out of the trap because the electric potential shown in Eq. (1.1) actually forms a hill, rather than a well, in the radial direction.

For these reasons we have developed an indirect detection scheme that utilizes radial position-sensitive, and therefore cyclotron and magnetron energy-sensitive, shifts in the axial frequency brought about by small anharmonic components in the trap's electric field. With this scheme we need only one tuned preamplifier to monitor the axial motion since the trap voltage can be adjusted to bring the axial oscillation frequency ω_z of any ion species into resonance. (This is true as long as the ion's motion remains stable [21], i.e., $\omega_m < \omega_c/2$.)

We will begin by describing the direct detection of the axial motion. Next we describe the anharmonic electrostatic C_4 term and how it couples the radial degrees of freedom into a measurable shift in the axial frequency. We then describe the detection method which beats a slightly off-resonant drive against the thermal Brownian motion at 4 K. Because of the possibly more general application of this "beating the noise" technique, we include a section that contains a thorough theoretical description. An appendix is added to give this description mathematical rigor. Discussion of the inherent systematic effects introduced by the necessary anharmonic coupling are scattered throughout the paper and summarized at the end where we suggest possible approaches that can be taken to minimize or eliminate these shifts.

II. AXIAL DETECTION

Detection of the axial motion is virtually identical to that used in the previous g-2 experiments and has been described extensively in previous articles [6,16,22]. We give here only a brief description primarily to define the axial temperature and the detection resolution.

The charged particle's axial motion induces an oscillation current of about 10^{-14} amp in the trap's end caps. The capacitance of one end cap to ground together with the inductance of a helical resonator form a tuned circuit. On resonance this tuned circuit's impedance is purely resistive and, if resonant with ω_z, it will damp the axial motion to the ambient temperature of the 4-K liquid-helium bath. These currents, and therefore the axial motion, are detected via the superheterodyne system shown schematically in Fig. 2.

A key feature of this system is the liquid-helium-cooled

GaAs field-effective transistor (FET) preamplifier whose noise temperature reflects the 4-K environment. This allows the phase-sensitive detector (PSD) to isolate a coherently driven axial motion that is smaller than the particle's thermal motion, assuming that the detection bandwidth is set narrower than the trapped particle's axial linewidth. We modulate the trap's electric well depth to generate FM sidebands in the axial motion. This enables us to isolate the drive signal, applied at one of these FM sidebands, from the narrow-band preamplifier which is tuned many linewidths away at the frequency of the fundamental axial motion. Finally, the PSD utilizes the phase relationship between the drive and the resulting motion of this harmonic oscillator to generate a synchronous axial resonance as shown in Fig. 3.

This dispersive resonance, referred to as the error signal, is used to frequency lock the axial motion via a voltage feedback to the trap's ring. In addition to stabilizing the axial motion and thereby the trapping fields, the feedback voltage also gives real-time information about changes in perturbations that affect the axial motion. For instance, a change in the radial position of the trapped charge due to a resonant cyclotron drive produces, via the small electric anharmonic coupling, a change in the axial "spring constant" which can be continuously monitored by recording the feedback voltage.

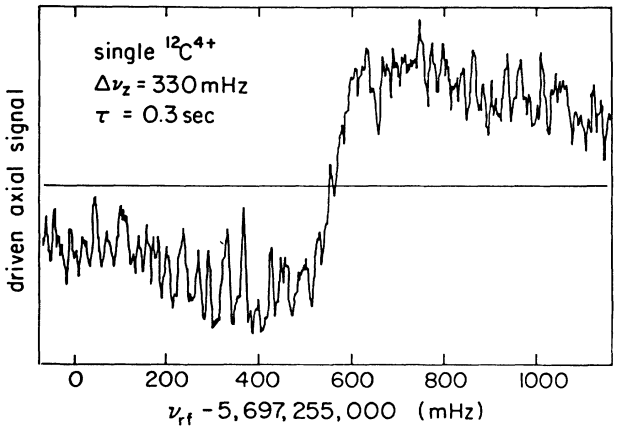

FIG. 3. The axial resonance of a single $^{12}C^{4+}$ ion taken with the apparatus shown in Fig. 2. A phase shift has been injected into the heterodyne to produce this dispersive shape which is appropriate as an error signal for the frequency lock.

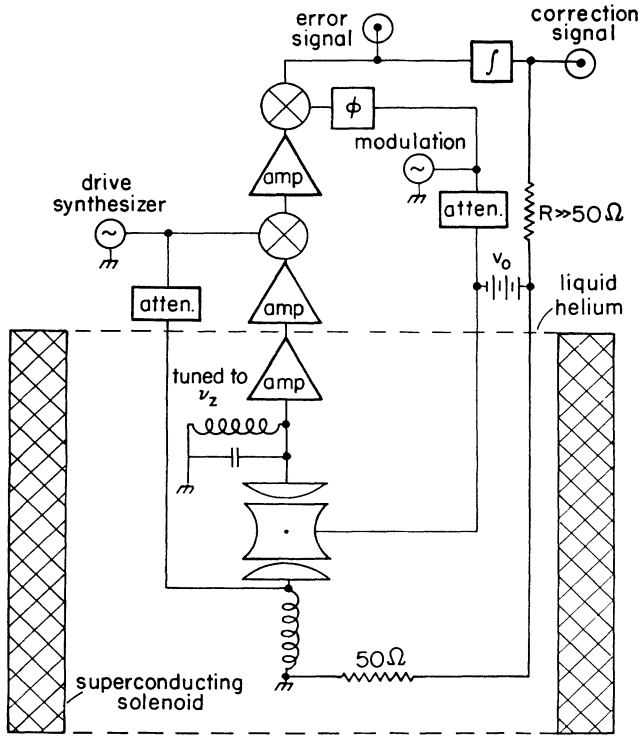

FIG. 2. Schematic of the axial-detection electronics. We drive the harmonic axial motion on a FM sideband via an rf drive applied to one end cap and then look at the induced currents in the other end cap that flow through a parallel tuned circuit, resonant at the fundamental axial frequency. The sidebands are generated by modulating the ring potential. The currents induced in the end cap are amplified by a GaAs FET transistor submersed in liquid helium, and then mixed to dc to display the phase relation between the drive and the driven axial motion. (See Fig. 3.) This phase relation is used as an error signal which is integrated and fed back to the ring voltage to frequency lock the axial motion to the drive source.

Assuming the trap to be truly harmonic, the fundamental limitation to the resolution of the axial resonance is due to the instability of the applied ring potential. This potential is produced by oven-controlled standard cells, and we experimentally observe voltage fluctuations of about 2×10^{-8} over times of less than one minute. We have also resolved changes in perturbations that induce relative shifts in the axial frequency on the order of $R_z=\Delta\omega_z/\omega_z\geq10^{-8}$. This sets the magnitude of the perturbation necessary for the anharmonic detection discussed in the next section. It should be noted, however, that these voltage fluctuations do *not* appear directly in either ω_c' or ω_m to the extent that the axial lock loop can correct for them to keep V_0 constant.

III. ANHARMONIC DETECTION

A real Penning trap, such as the one shown in Fig. 1, does not produce a pure quadratic potential. We can, however, approximate the real potential in an expansion which contains the trap's basic rotational and reflection symmetries with respect to the z axis,

$$V=\frac{V_0}{2}\sum_{k=0}^{\infty}C_{2k}\left[\frac{r}{d}\right]^{2k}P_{2k}(\cos\theta)\ . \tag{3.1}$$

In this expansion r is much less than d for a single charge in a typical Penning trap at 4 K, assuming that sideband cooling [6] has been used to reduce the magnetron radius. We are therefore justified in keeping only the first term beyond the leading quadratic approximation. Rewriting the Legendre polynomial in cylindrical coordinates gives

$$V = V_0 \left[\frac{z^2 - \rho^2/2}{2d^2} \right] + V_0 C_4 \left[\frac{z^4 - 3z^2\rho^2 + 3\rho^4/8}{2d^4} \right] . \tag{3.2}$$

Here we have incorporated C_2 into V_0 to recover Eq. (1.1) as the leading term. The z^4 term induces a shift in the axial frequency that is quadratic in z or linear in the axial energy. We use this shift as an indicator of the size and sign of the C_4 term. By changing the potential of the guard voltage (see Fig. 1) relative to the ring voltage, we can change C_4. In theory there will exist a guard voltage at which C_4 vanishes. At this guard voltage successively harder axial drives will not induce anharmonic frequency shifts in the axial resonance until a higher-order term begins to dominate. These higher-order electrostatic terms are minimized by using hyperbolic electrodes [23] rather than some other cylindrically symmetric geometry [24] such as cylinders and plates. With the guard voltage set to either side of this C_4 null, the axial resonance will show anharmonic pulling with successively harder drives as shown in Fig. 4.

The $\rho^2 z^2$ term adds to the axial well depth a shift that is quadratic in ρ or linear in the radial energies. This term generates a shift in the axial frequency, and therefore a shift in the ring's feedback voltage when we induce changes in the cyclotron and magnetron energies with resonant drives. This is the anharmonic detection to which we have referred. Finally, there are shifts in the cyclotron and magnetron frequencies resulting from the $\rho^2 z^2$ and ρ^4 terms that can introduce serious systematic errors.

A detailed calculation for the anharmonic frequency shifts due to the C_4 perturbation has been performed previously [17]. This can be accomplished in a straightforward manner by rewriting the C_4 perturbation in terms of the creation and annihilation operators of the fundamental oscillator motions and then applying first-order perturbation theory. We present the calculated shifts parametrized in terms of two constants,

$$\alpha = \frac{\omega_z}{\omega_c'} \approx \frac{\omega_z}{\omega_c} \quad \text{and} \quad \beta = \frac{6C_4}{eV_0} . \tag{3.3}$$

Here α characterizes the relative strengths of the trapping electric and magnetic fields, while β is proportional to the C_4 perturbation which is a function of the guard compensation voltage.

The calculated shift in the axial frequency, representing the *signal* in the anharmonic-detection scheme, is given to leading order in α by

$$\frac{\Delta\omega_z(C_4)}{\omega_z} = \beta\left(-\tfrac{1}{2}\alpha^2 E_c + \tfrac{1}{4}E_z + E_m\right) . \tag{3.4}$$

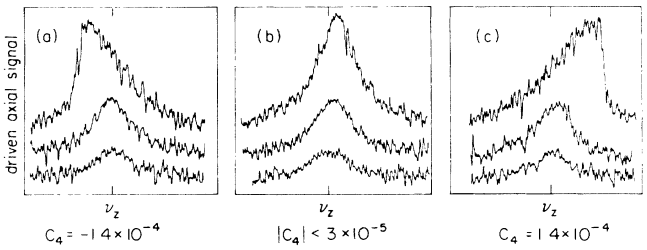

FIG. 4. These axial resonances were taken using a few protons with a phase shift injected into the heterodyne to produce an absorption line shape, a $\pi/2$ shift from the dispersive shape shown in Fig. 3. (a) In this set of resonances the guard voltage has been set to produce a negative value for C_4; anharmonic pulling down in frequency under successively harder axial drives can be seen. (c) In this set of resonances the guard voltage has been set to produce a positive C_4 thereby changing the direction of anharmonic pulling. (b) By monitoring this anharmonic pulling while changing the guard voltage we can minimize C_4 and produce axial resonances which show no anharmonic pulling under successively harder drives. Comparing the change in guard voltage (around this null) over which no anharmonic pulling is seen, and using a relaxation calculation for C_4 changes as a function of guard voltage [25], we find that $C_4 < 3\times10^{-5}$ at this null.

Figure 5(a) shows a typical cyclotron resonance taken via a ΔE_c induced shift in the axial frequency. This power-broadened resonance was taken with the low power of ≈ -140 dBm capacitively coupled through 50 Ω to opposite quadrants of the split quadring electrode shown in Fig. 5(b). The axial lock is monitored while this drive is swept up in frequency through the cyclotron resonance. On resonance, cyclotron energy is absorbed producing a shift in the feedback voltage to correct for the perturbation described in Eq. (3.4). The drive is then turned off and the cyclotron motion is allowed to cool back into equilibrium with a weakly coupled resistor at 4 K [one of the low Q tuned circuits shown in Fig. 5(b)]. The drive is then turned on again and swept from the opposite direction to bracket the cyclotron resonance.

A resolution of $\Delta\omega_c'/\omega_c' \approx 10^{-10}$ has been achieved for resonances taken with this approach. To get an estimate of the inherent systematics introduced by the C_4 perturbation, which is fundamental to detection, we must also look at the calculated [17] shifts in the cyclotron and magnetron frequencies. They are, again to leading order in α,

$$\frac{\Delta\omega_c'(C_4)}{\omega_c'} = \beta\alpha^2\left(\tfrac{1}{4}\alpha^2 E_c - \tfrac{1}{2}E_z - E_m\right) \tag{3.5}$$

and

$$\frac{\Delta\omega_m(C_4)}{\omega_m} = \beta\left(-\alpha^2 E_c + E_z + E_m\right) . \tag{3.6}$$

These calculations assume the ring potential is fixed. In the experiment, however, the axial frequency is not allowed to change. It is held constant by changing the ring potential as explained in the section on axial detection. This will induce an additional shift in ω_c' and ω_m as C_4 is increased from zero. To compute these shifts, we first differentiate Eq. (1.5) with respect to ω_z and neglect the small correction of order α^2 in the variation of ω_c' to obtain

$$\frac{\Delta\omega_m(\text{lock})}{\omega_m} = -2\frac{\Delta\omega_z(C_4)}{\omega_z} . \tag{3.7}$$

Then the relation $\omega_c' = \omega_c - \omega_m$ gives to this leading order

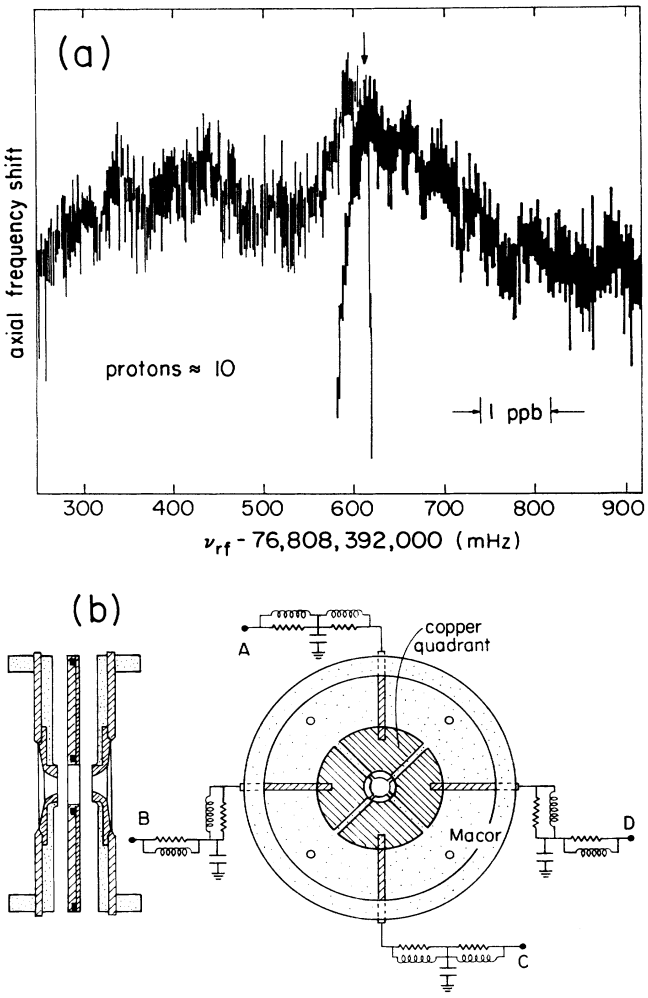

FIG. 5. (a) The cyclotron resonance of a small cloud of protons, taken via anharmonic detection with 0.1 ppb resolution. (b) The hyperbolic quadring contains four electrically isolated copper electrodes which are rigidly attached to a macor substrate to maintain cylindrical symmetry. An rf drive applied across opposite quadrants (A and C) is swept through the cyclotron frequency both from below resonance and from above. On resonance, energy is absorbed inducing a sudden shift in the axial feedback voltage which is displayed (a). The points of initiation of the initial axial shift (or triggered response) identify the maximum limits of the resonant frequency. When the rf drive is off, the cyclotron motion comes back into thermal equilibrium ($\tau_{1/2} \approx 10$ min.) with the low-Q tuned circuits at a temperature of 4 K. These tuned circuits are formed by resonating the ~ 4 pF capacitance between each ring quadrant and ground with inductors shorted to ground through 680 pF. The electrical points A, B, C, and D, and therefore the quadrants of the ring electrode, are shorted together at the magnetron frequency to give a high-conductance path for the image currents associated with the magnetron motion. Because the magnetron motion is unstable, substantial resistive losses in the ring electrode would drive the ions radially out of the trap.

$$\frac{\Delta\omega_c'(\text{lock})}{\omega_c'} = \alpha^2\frac{\Delta\omega_z(C_4)}{\omega_z} . \tag{3.8}$$

Combining these lock-induced shifts with the original shifts due to C_4 gives the total observed systematic shifts for a C_4 perturbation under the experimental conditions of an axial lock

$$\frac{\Delta\omega_z(C_4+\text{lock})}{\omega_z} \equiv 0 , \tag{3.9}$$

$$\frac{\Delta\omega_c'(C_4+\text{lock})}{\omega_c'} = -\beta\frac{\alpha^2}{4}(\alpha^2 E_c + E_z) , \tag{3.10}$$

$$\frac{\Delta\omega_m(C_4+\text{lock})}{\omega_m} = \beta\left[\frac{E_z}{2} - E_m\right] . \tag{3.11}$$

Although we have not displayed the algebra here for this first-order (C_4) perturbation calculation, one can show that E_m does not appear on the right-hand side of Eq. (3.10) to all orders in α and similarly E_c does not appear in Eq. (3.11) to any order in α.

This simple expedience of using lock-induced shifts for absolute energies is done to simplify equations later. It in no way changes the value of the free-space cyclotron frequency ω_c obtained by using the quadrature invariance equation (1.6), since this equation is not changed by variations in the trapping potential. It does, however, reflect the experimentally observable changes in ω_c' and ω_m when corresponding changes occur in the trapped ion's various energies and/or in C_4. It should be noted that the axial-lock time constant is set long in order to stabilize the loop. If energy is absorbed at too fast of a rate, the loop will lose lock. In that case one should revert back to using Eqs. (3.4)–(3.6); however, the analysis becomes difficult because equilibrium conditions no longer exist. The basic difference between the two cases is that anharmonic pulling of the cyclotron frequency changes sign and detection sensitivity may be altered (though, under certain conditions, systematics might be legitimately estimated by assuming only the values of E_c, E_z, and E_m prior to the interrogation of the cyclotron resonance).

For the remainder of this paper we will assume that the trapped ion has a mass-to-charge ratio of three. This represents $^3H^+$, which is the most difficult atom to deal with in our trap because it cannot be multiply charged to give an increased signal-to-noise ratio [2,14]. A $^3H^+$ ion in our trap in a 5-T magnetic field with 40 V on the quadring electrode has a cyclotron frequency $\omega_c \approx 26$ MHz and an axial frequency $\omega_z \approx 5$ MHz. This gives a value of $\alpha \approx 0.2$.

As explained earlier, we can resolve relative shifts in the axial frequency given by $R_z = \Delta\omega_z/\omega_z \approx 10^{-8}$. Therefore, via Eq. (3.4), the onset of detection will occur when the cyclotron energy has increased such that

$$R_z = \frac{\beta\alpha^2}{2}\Delta E_c \approx 10^{-8} . \tag{3.12}$$

If we then assume that this increased cyclotron energy dominates in Eq. (3.10), the C_4 induced systematic shift

in the cyclotron frequency becomes

$$\frac{\Delta\omega_c'(C_4+\text{lock})}{\omega_c'} \approx \frac{\alpha^2}{2} R_z = 2\times 10^{-10} \tag{3.13}$$

at the onset of detection.

To validate our assumption that the cyclotron energy dominates in Eq. (3.10), we must estimate the size of β to determine ΔE_c at the onset of detection via Eq. (3.12). The value of β can be estimated by comparing the experimental width of the guard voltage over which C_4 is minimized (as determined by the method described earlier), with an electrostatic relaxation calculation [25] that predicts changes in C_4 for a given change in the guard voltage. For our trap this relaxation calculation predicts

$$\Delta C_4 = \frac{\Delta V_g}{V_0} 1.4\times 10^{-2} , \tag{3.14}$$

where ΔV_g represents the change in the voltage applied to the guard electrodes shown in Fig. 1.

Our guard nulls typically determine $\Delta V_g / V_0$ to within ± 0.002, which predicts an uncertainty in the null of C_4 at $\Delta C_4 \approx 2.8\times 10^{-5}$. Using this and a ring voltage of $V_0 = 40$ V gives $\beta \approx 4\times 10^{-6}$ $(\text{eV})^{-1}$ or, via Eq. (3.12), an estimate of $\alpha^2 \Delta E_c \approx 5\times 10^{-3}$ eV at the onset of detection. This certainly dominates over the 3×10^{-4} eV thermal energy of the 4-K axial motion validating our original assumption and therefore the systematics estimated in Eq. (3.13). Note that β can be increased to about 5×10^{-5} $(\text{eV})^{-1}$ with no noticeable increase in the C_4 induced systematic. This has the benefit of lowering the change in cyclotron energy necessary for anharmonic detection through the axial motion and therefore lowering systematics due to other perturbations such as a magnetic gradient and relativistic effects which also scale with the trapped particle's energy. For $\beta > 5\times 10^{-5}$ $(\text{eV})^{-1}$ the axial energy at a temperature of 4 K begins to contribute to the systematics described by Eq. (3.10).

The systematic described by Eq. (3.13) is *fundamental* to anharmonic detection and assumes that the C_4 perturbation dominates. It is possible that there exist other energy-dependent perturbations that produce anharmonic shifts in the axial motion [16,17]. If this is the case, then, the guard voltage null (obtained by minimizing the axial shifts produced by successively harder axial drives) represents a cancellation of the C_4 perturbation against these other perturbations under changes in the axial energy only. In general, C_4 would not be nulled out in this case and we would therefore expect a different systematic shift in the measured cyclotron frequency.

The systematic associated with anharmonic detection scales as $\alpha^2 R_z$ and can therefore be reduced by reducing ω_z or increasing ω_c. We currently use a single-filament superconducting magnet which has a maximum field of 6 T. This is typically the highest *stable* magnetic field that can be reached. Multifilament superconducting magnets can reach fields approaching 10 T but in general are not as stable as the single-filament magnets, although stable multifilaments magnets are known to exist [4]. Persistent magnets with fields as high as 20 T have recently become commercially available [26]; however they also suffer from field-stability problems in addition to poor homogeneity. We conclude that increasing ω_c will be difficult. Therefore, the most straightforward way to reduce α^2 would be to reduce the potential on the ring, thereby reducing the axial frequency. Unfortunately, this would make the trap more susceptible to asymmetrical surface charging and patch effects that reduce the harmonic volume of the trap, thus making it difficult to resolve the axial resonance at the 10^{-8} level. (For instance, the higher-order C_6 term may come into play.) Fortunately, studies [27] have indicated that patch effects on surfaces at 4 K can be drastically reduced with the use of graphite and gold coatings. We can also reduce ω_z by increasing the size of the trap. This will decrease the coupling of the trapped ion to the axial detection making it more difficult to detect and resolve a single ion whose linewidth will be narrower and therefore more susceptible to fluctuations in the ring potential. This decrease in coupling can be counteracted by working with multiply charged ions [2,14,28] or by developing higher-Q tuned circuits [29] in the detection front end. It might also be possible to replace the oven-controlled standard cells with a zero-bias series array Josephson voltage standard which can reach tens of volts and show voltage stabilities comparable to the 70-GHz source that drives it [30]. Another possibility is to use the voltage on the ring of a reference trap [31] with a trapped ion whose axial frequency has been locked to an ultrastable frequency synthesizer.

A reduction in α^2 and therefore the inherent systematics associated with anharmonic detection below 0.1 ppb is apparently possible. In addition, with a more stable voltage source the axial resolution R_z may be improved which effectively increases the signal in the anharmonic detection scheme. This reduces the minimum energy changes needed for detection and therefore the systematics associated with these changes.

We have ignored the systematic introduced into the magnetron frequency by the C_4 perturbation. This is because relative errors in the magnetron frequency are reduced by the factor of $\alpha^4/4 \approx 4\times 10^{-4}$ when used in Eq. (1.6) to predict the free-space cyclotron frequency. This can be seen by differentiating this quadrature invariance equation to obtain

$$\frac{\delta\omega_c}{\omega_c} = \left[\frac{\omega_c'}{\omega_c}\right]^2 \frac{\delta\omega_c'}{\omega_c'} + \left[\frac{\omega_z}{\omega_c}\right]^2 \frac{\delta\omega_z}{\omega_z} + \left[\frac{\omega_m}{\omega_c}\right]^2 \frac{\delta\omega_m}{\omega_m} , \tag{3.15}$$

which on substituting $\alpha = \omega_z/\omega_c'$, gives to leading order in α

$$\frac{\delta\omega_c}{\omega_c} = \frac{\delta\omega_c'}{\omega_c'} + \alpha^2 \frac{\delta\omega_z}{\omega_z} + \frac{\alpha^4}{4} \frac{\delta\omega_m}{\omega_m} . \tag{3.16}$$

Nonetheless, the C_4 induced shifts in the magnetron frequency described by Eq. (3.11) can be large and easily observable. Figure 6 shows the observed shift in the magnetron frequency as a function of β. Using the slope of the

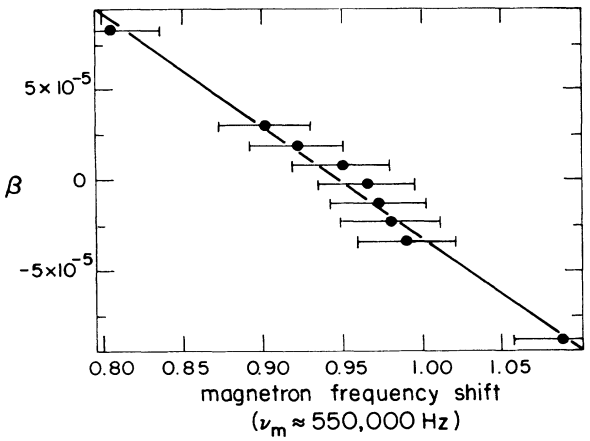

FIG. 6. Experimentally observed shift in the magnetron frequency of a single $^{12}C^{4+}$ ion as a function of β (guard voltage). The magnetron energy can be estimated from the slope of this graph and is $E_m \approx 4\times 10^{-3}$ eV, which is about 100 times the minimum energy predicted by sideband cooling.

graph in Fig. 6 and ignoring the axial energy in Eq. (3.11) we get an estimate for the magnetron energy of $E_m \approx 4\times 10^{-3}$ eV. Interestingly, this is about 100 times the minimum energy predicted by side-band cooling theory [6] but is in better agreement than other minimum magnetron energy measurements obtained independently in two other Penning traps using electrons; these other traps have shown a discrepancy [22,32] of about a factor of 400 to 600. Fortunately this larger than expected magnetron energy does not enter into the C_4 systematic shift of ω_c' because the axial energy at 4 K still dominates [see Eq. (3.10)]. The magnetron energy's relative contribution to C_4 induced errors in the predicted free-space cyclotron frequency can be shown to be on the order of 0.005 ppb. To do this, we insert the locked frequency shifts given by Eqs. (3.10) and (3.11) into Eq. (3.16) to obtain to leading order in α

$$\frac{\delta\omega_c}{\omega_c} \approx -\frac{\beta\alpha^4}{4}\left[E_c + \frac{1}{\alpha^2}E_z + E_m\right] . \tag{3.17}$$

Since the quadrature invariance equation is not altered by changes in the trapping potential, this result also holds for the unlocked case as well. Here we have assumed that E_c, E_z, and E_m are unchanged for the measurement of ω_c' and ω_m. This larger magnetron energy can, however, affect ω_c' through other perturbations, in particular, that of a magnetic gradient; however, these perturbations are not fundamental to the detection schemes discussed here and thus will be ignored.

Energy adsorbed during excitation of the cyclotron motion is damped out via a weak coupling of the ion's image currents to a resistor at 4 K (see Fig. 5). The value of the resistor has been chosen to produce radiative linewidths of approximately 0.1 ppb in relative width. As a result, it typically takes more than 20 minutes for the cyclotron motion to return to equilibrium with the resistor after adsorbing enough energy to observe resonances of the type shown in Fig. 5(a). This equilibration must be accomplished if we wish to minimize systematic errors before we begin the sweep from the opposite direction that brackets ω_c'. Even if side-band cooling at $\omega_c' - \omega_z$ is used to speed up equilibration time, we will spend several minutes sweeping out the resonance and only a few seconds absorbing drive energy. We therefore spend only a small fraction of the total time actually interrogating the resonance and this is a poor approach to maximizing the signal-to-noise ratio.

A less destructive method of continuously interrogating the cyclotron resonance was therefore developed. This method takes advantage of the long coherence time $1/\gamma_c$ of the cyclotron Brownian motion (due to a thermal white noise drive) by beating this motion at ω_c' against that due to a slightly off-resonant coherent drive at $\omega_d = \omega_c' + \Delta\omega$. The beauty of this technique is that E_c oscillates continuously at this difference frequency $\Delta\omega$. This in turn induces a modulation in the axial-lock voltage via the C_4 perturbation as described in Eq. (3.4) and the previous discussion on anharmonic detection. Knowing the drive frequency and monitoring the beat frequency then gives a continuous monitor of ω_c'.

An analogous way to visualize the process is to treat the harmonic cyclotron motion as a narrow-band filter centered at ω_c' with a linewidth of γ_c. This "filter" then picks out of the thermal white noise drive a signal centered at ω_c' with a width of γ_c or a coherence time of $1/\gamma_c$. This signal then beats against the off-resonant coherent drive signal, which comes through the "filter" at some level.

This technique is demonstrated in Fig. 7 which shows a small 4-minute section of beating observed in the axial-lock voltage that was continuously monitored for $\approx \frac{1}{3}$ h. The frequency resolution of this 4-min section, obtained by measuring the separation between successive peaks, approaches 10^{-11} relative to ω_c'. An electronic Fourier transform will give a more precise measure of the resonant frequency. Also, a reference oscillator can be locked

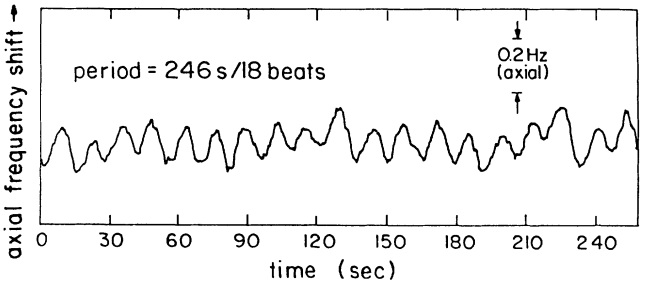

FIG. 7. The feedback voltage in the axial lock is observed to beat continuously at the difference frequency between a coherent off-resonant drive and the resonant frequency of the cyclotron motion of a single $^{12}C^{4+}$ ion. The feedback voltage is a monitor of the cyclotron energy via the C_4 perturbation. This beat signal is resolved to within 0.01 ppb relative to the cyclotron frequency.

to the beat or vice versa in order to determine the resonant frequency.

A discussion of the inherent systematic in this technique requires an understanding of the actual amplitude of the oscillating cyclotron energy in addition to the average cyclotron energy. This will be calculated in the next section. We would like however, to stress that we have demonstrated a technique that continuously monitors ω_c' with the phenomenal resolution of 10^{-11}.

IV. BEATING THE NOISE—THEORY

The cyclotron velocity is the sum of two parts. One part is the velocity $\mathbf{u}(t)$ which describes the Brownian motion brought about by the weak coupling of the charged particle with its thermal environment at temperature T. Since this coupling to an effective thermal bath is very feeble, the corresponding relaxation rate γ_c is very small in comparison to the cyclotron frequency ω_c', $\gamma_c \ll \omega_c'$. Over times that are short in comparison to $1/\gamma_c$, the thermal velocity $\mathbf{u}(t)$ goes about a circle at frequency ω_c'. Over times on the order of $1/\gamma_c$, the magnitude and phase of $\mathbf{u}(t)$ vary in a random fashion. Thus the thermal or noise energy

$$E_N(t)=\tfrac{1}{2}m\,\mathbf{u}(t)^2 \tag{4.1}$$

varies slowly; it varies significantly only in a time set by the scale $1/\gamma_c$. On the average,

$$\langle E_N(t)\rangle = k_B T\ , \tag{4.2}$$

in accord with the equipartition theorem. It is convenient to think of this average as a thermal ensemble average—an average over many identical copies of the system, but the average is also the average over times that are long in comparison with $1/\gamma_c$. The other part of the cyclotron motion has the velocity $\mathbf{v}(t)$ brought about by an external, coherent drive. This velocity goes about a circle with the drive frequency ω_d with its magnitude fixed (as long as the drive is continued). Thus the energy

$$E_D=\tfrac{1}{2}m\,\mathbf{v}(t)^2 \tag{4.3}$$

is constant. The experiment measures the total energy $E(t)$ in the cyclotron motion,

$$\begin{aligned} E(t)&=\tfrac{1}{2}m\,[\mathbf{u}(t)+\mathbf{v}(t)]^2 \\ &=E_N(t)+E_D+E_B(t)\ , \end{aligned} \tag{4.4}$$

in which

$$E_B(t)=m\,\mathbf{u}(t)\cdot\mathbf{v}(t)\ . \tag{4.5}$$

Basically, $\mathbf{u}(t)$ and $\mathbf{v}(t)$ go about circles with a frequency difference

$$\Delta\omega=\omega_d-\omega_c'\ . \tag{4.6}$$

This basic motion is altered by the fluctuations in the thermal velocity $\mathbf{u}(t)$ and so

$$E_B(t)=2\sqrt{E_D E_N(t)}\cos[\Delta\omega t+\theta(t)]\ . \tag{4.7}$$

The relative phase $\theta(t)$ varies significantly during times on the order of $1/\gamma_c$ as does $E_N(t)$. However, the thermal coupling is so weak that $\gamma_c \ll \Delta\omega$, and the beats described by $E_B(t)$ are prominent.

The beating never ceases. But the phase and amplitude coherence between beats that are separated by a long time interval t_1, $t_1 > 1/\gamma_c$, is destroyed by the slow random fluctuations of the thermal motion. Therefore, the beat frequency $\Delta\omega$ (and from it the cyclotron frequency ω_c') can be measured with a linewidth on the order of γ_c. To place this linewidth problem in quantitative terms, let us suppose that the Fourier transform of the signal is constructed from measurements made over a very long interval $2t_0 \gg 1/\gamma_c$. Subtracting out the average background, this Fourier transform is given by

$$E(\omega)=\frac{1}{\sqrt{2t_0}}\int_{-t_0}^{t_0} dt\, e^{i\omega t}F(t)\ , \tag{4.8}$$

where

$$F(t)=E_N(t)-k_B T+E_B(t)\ . \tag{4.9}$$

The average over many experimental runs is the same as the thermodynamic ensemble average. This average of $F(t)$ vanishes and so

$$\langle E(\omega)\rangle = 0\ . \tag{4.10}$$

The proper measure of the linewidth is given by the average of the absolute square of the Fourier transform $|E(\omega)|^2$. The detailed calculation in the Appendix shows that

$$\begin{aligned} \langle |E(\omega)|^2\rangle &= (k_B T)^2\frac{2\gamma_c}{\omega^2+\gamma_c^2} \\ &\quad +(k_B T)E_D\left[\frac{\gamma_c}{(\omega-\Delta\omega)^2+\gamma_c^2/4}\right. \\ &\quad \left.+\frac{\gamma_c}{(\omega+\Delta\omega)^2+\gamma_c^2/4}\right]\ . \end{aligned} \tag{4.11}$$

The first term on the right-hand side of this result simply describes the noise in the nondriven cyclotron motion; the second set of terms describe the beating signal—a Lorentzian line shape peaked at $\omega=\Delta\omega$ with a full width at half maximum given by γ_c. Taking a drive amplitude to give a coherent excitation on the order of the thermal noise $E_D \approx k_B T$ and evaluating the Fourier transform at the peak $\omega=\Delta\omega$, we see that the level of the background noise of the nondriven cyclotron motion relative to the beating signal is on the order of $(\gamma_c/\Delta\omega)^2$, the same order as the contribution of the counter-rotating beat signal (the last Lorentzian peaked at $\omega=-\Delta\omega$). These are very small backgrounds.

We have now explained the essential aspects of the beat signal. However, since the technique is a novel one—it is unusual to perform a precise experiment by beating a coherent drive with thermal noise—a more detailed statistical description is warranted. This we do now.

Since the relaxation time $1/\gamma_c$ of the cyclotron motion

to its thermal environment at temperature T is so long, an initial measurement of this motion can be made, and this is effectively performed in the experiment. This measurement picks out the particular state of the thermal ensemble which the motion happens to be in at the initial time. To see what this implies, we first consider the nondriven motion. Then, as shown in the Appendix, the conditional probability density for observing the velocity $\mathbf{u}$ at a later time t given that the initial velocity at time $t=0$ is $\mathbf{u}_0$ is given by

$$P_{\mathbf{u}_0}(\mathbf{u},t)=\left[\frac{m}{2\pi k_B T}\right]\frac{1}{1-e^{-\gamma_c t}} \times\exp\left[-\frac{m}{2k_B T}\frac{[\mathbf{u}-e^{-\gamma_c t/2}\mathbf{u}_0(t)]^2}{1-e^{-\gamma_c t}}\right] . \tag{4.12}$$

Here $\mathbf{u}_0(t)$ is the velocity that an undamped particle would have at time t if it had the initial velocity $\mathbf{u}_0$ at time $t=0$. The velocity $\mathbf{u}_0(t)$ is just the original velocity $\mathbf{u}_0$ rotated at the cyclotron frequency ω_c'. In the limit $t\to 0$, the Gaussian form produces a representation of the δ function,

$$P_{\mathbf{u}_0}(\mathbf{u},t)\to\delta(\mathbf{u}-\mathbf{u}_0(t)),\quad t\to 0 . \tag{4.13}$$

For times that are short in comparison with the damping time $1/\gamma_c$, the probability is sharply peaked about the classical trajectory $\mathbf{u}_0(t)$. At longer times, the fluctuations brought about by the interaction of the cyclotron motion with the thermal bath come into play, and the probability of finding a velocity $\mathbf{u}$ broadens. Finally, for long times, the probability distribution relaxes to the Maxwell-Boltzmann form, and the particular initial velocity is forgotten,

$$P_{\mathbf{u}_0}(\mathbf{u},t)\simeq\left[\frac{m}{2\pi k_B T}\right]\exp\left[\frac{-m\mathbf{u}^2}{2k_B T}\right],\quad t\gg 1/\gamma_c . \tag{4.14}$$

The observed energy is given by

$$E(t)=\tfrac{1}{2}m[\mathbf{v}(t)+\mathbf{u}]^2 . \tag{4.15}$$

This is the case for a particular thermal velocity $\mathbf{u}$. If this velocity is measured to be $\mathbf{u}_0$ at time $t=0$, then its probable value is distributed over a range of velocities at a later time t given by $P_{\mathbf{u}_0}(\mathbf{u},t)$. Hence the probability density for observing the energy E at time t is expressed as

$$P_{\mathbf{u}_0}(E,t)=\int(d^2\mathbf{u})\delta(E-\tfrac{1}{2}m[\mathbf{v}(t)+\mathbf{u}]^2)P_{\mathbf{u}_0}(\mathbf{u},t) . \tag{4.16}$$

For small times $P_{\mathbf{u}_0}(\mathbf{u},t)\simeq\delta[\mathbf{u}-\mathbf{u}_0(t)]$, and so

$$P_{\mathbf{u}_0}(E,t)\simeq\delta(E-\tfrac{1}{2}m[\mathbf{v}(t)+\mathbf{u}_0(t)]^2),\quad t\to 0 . \tag{4.17}$$

Since, at least in principle, $\mathbf{v}(t)$ is known, this initial energy distribution with the measurement of the energy at $t=0$ and a short while later determines the particular starting velocity $\mathbf{u}_0$. Then, armed with this initial information, $P_{\mathbf{u}_0}(E,t)$ gives the distribution of energies that will be observed at later times. [To simplify this discussion, we assume that $\mathbf{u}_0$ is precisely known. In fact, there is an error in determining $\mathbf{u}_0$ because the distribution spreads a little at the short, later time $\simeq 1/\Delta\omega$ needed to fix both the magnitude and phase of $\mathbf{u}_0$. In view of Eq. (4.28), with $E_D\simeq E_N=k_B T$, $\Delta u/u\simeq\Delta E/E\simeq\sqrt{\gamma_c/\Delta\omega}$.]

It is not difficult to explicitly compute the energy distribution at all times. This is accomplished by first changing integration variables to $\mathbf{u}'=\mathbf{v}(t)+\mathbf{u}$, integrating with polar coordinates in the new variables, and using formula (4.12) for $P_{\mathbf{u}_0}(\mathbf{u},t)$,

$$P_{\mathbf{u}_0}(E,t)=\left[\frac{m}{2\pi k_B T}\right]\frac{1}{1-e^{-\gamma_c t}}\int_0^{2\pi}d\phi\int_0^{\infty}u'du'\delta(E-\tfrac{1}{2}mu'^2)\exp\left[-\frac{m}{2k_B T}\frac{u'^2+w^2-2u'w\cos\phi}{1-e^{-\gamma_c t}}\right] . \tag{4.18}$$

Here

$$\mathbf{w}(t)=\mathbf{v}(t)+e^{-\gamma_c t/2}\mathbf{u}_0(t) , \tag{4.19}$$

and the polar angle ϕ has been chosen to be the angle between the two vectors $\mathbf{u}'$ and $\mathbf{w}$. The radial u' integral is trivial because of the δ function. The angular ϕ integral defines the imaginary Bessel function $I_0(z)$. To put the result in a neat form, we define

$$\mathcal{E}(t)=\tfrac{1}{2}m\mathbf{w}(t)^2 . \tag{4.20}$$

Then

$$P_{\mathbf{u}_0}(E,t)=\frac{1}{k_B T}\frac{1}{1-e^{-\gamma_c t}}\exp\left[-\frac{1}{k_B T}\frac{E+\mathcal{E}(t)}{1-e^{-\gamma_c t}}\right] \times I_0\left[\frac{2\sqrt{E\mathcal{E}(t)}}{k_B T(1-e^{-\gamma_c t})}\right] . \tag{4.21}$$

This expression may be simplified if the argument of the Bessel function is large, which happens for very small times $t\ll 1/\gamma_c$, or if the excitation energy is large $\mathcal{E}(t)\gg k_B T$. In this case, one may use the asymptotic form of the Bessel function to obtain

$$P_{\mathbf{u}_0}(E,t)\simeq[4\pi k_B T(1-e^{-\gamma_c t})\sqrt{E\mathcal{E}(t)}]^{-1/2} \times\exp\left[-\frac{1}{k_B T}\frac{[\sqrt{E}-\sqrt{\mathcal{E}(t)}]^2}{1-e^{-\gamma_c t}}\right] . \tag{4.22}$$

For small t this distribution is sharply peaked about $E=\mathcal{E}(t)$ and in the limit $t\to 0$ it becomes a representation of $\delta(E-\mathcal{E}(t))$.

In terms of the drive and initial "noise" energies,

$$\mathcal{E}(t)=E_D+E_N e^{-\gamma_c t}+2\sqrt{E_D E_N}e^{-\gamma_c t/2}\cos(\Delta\omega t+\theta) , \tag{4.23}$$

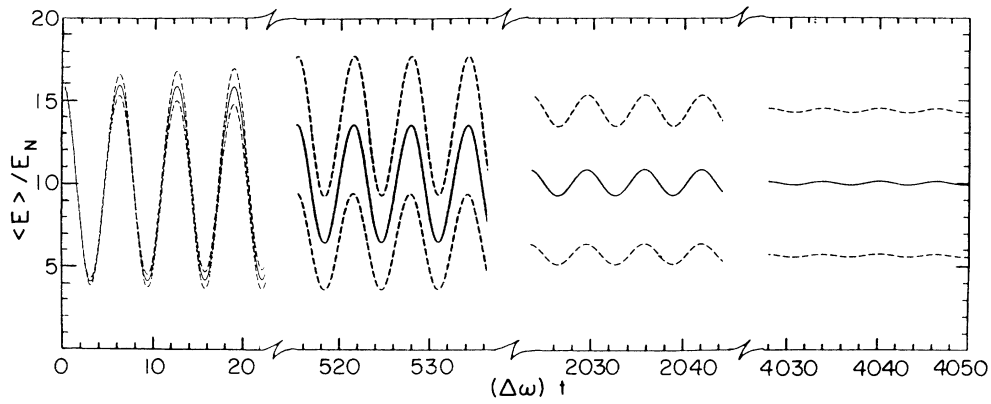

FIG. 8. The cross term in the cyclotron energy involving the product of thermal and driven velocities produces a beat signal in the energy that persists indefinitely. However, the signal loses phase and amplitude coherence between portions which are separated at time intervals that are larger than the cyclotron thermal relaxation time $1/\gamma_c$. This lack of coherence over long-time intervals is exhibited here by plotting the *average* signal which would be found over many experimental runs, each of which starts with the same initial conditions. An unrealistically large value of the damping constant γ_c is used so as to be able to show the effect. The dashed curves have the time-dependent rms energy fluctuation $\Delta E(t)$ added to and subtracted from this average energy.

where θ is the initial phase. Although we have the complete probability distribution $P_{\mathbf{u}_0}(E,t)$ in hand, the average energy that will be observed at time t,

$$\langle E\rangle_{\mathbf{u}_0}=\int dE\, E P_{\mathbf{u}_0}(E,t)\ , \tag{4.24}$$

(assuming that the thermal velocity is determined to be $\mathbf{u}_0$ at $t=0$) together with the squared fluctuation

$$\Delta E^2=\langle (E-\langle E\rangle_{\mathbf{u}_0})^2\rangle_{\mathbf{u}_0}$$

$$=\int dE(E^2-\langle E\rangle_{\mathbf{u}_0}^2)P_{\mathbf{u}_0}(E,t)\ , \tag{4.25}$$

give a clear description of the beating phenomena. An arbitrary energy moment is easily computed by returning to relation (4.16) between the energy and velocity distribution which gives

$$\int dE\, E^m P_{\mathbf{u}_0}(E,t)=\int (d^2\mathbf{u})\{\tfrac{1}{2}m[\mathbf{u}+\mathbf{v}(t)]^2\}^m P_{\mathbf{u}_0}(\mathbf{u},t)\ . \tag{4.26}$$

The resulting Gaussian integrations are readily performed, and one finds that

$$\langle E\rangle_{\mathbf{u}_0}=k_BT(1-e^{-\gamma_c t})+\mathcal{E}(t)\ , \tag{4.27}$$

and

$$\Delta E^2=k_BT(1-e^{-\gamma_c t})[k_BT(1-e^{-\gamma_c t})+2\mathcal{E}(t)]\ . \tag{4.28}$$

For times that are short in comparison with the cyclotron decay time $\gamma_c t\ll 1$, $\langle E\rangle_{\mathbf{u}_0}\simeq\mathcal{E}(t)$, which according to Eq. (4.23) displays beats at the frequency $\Delta\omega$. Moreover, for these short times, the spread in the observed energies $\Delta\mathcal{E}$ is very small. On the other hand, at long times, $\gamma_c t\gg 1$, $\mathcal{E}(t)\simeq E_D$, and the beats are washed out with $\langle E\rangle_{\mathbf{u}_0}\simeq k_BT+E_D$ and an energy dispersion of the same order, $\Delta E^2\simeq k_BT(k_BT+2E_D)$ appears.

The initial noise energy is distributed with the usual Maxwell-Boltzmann factor $\exp(-E_N/k_BT)$, and so E_N will typically be on the order of k_BT. In Fig. 8 we plot $\langle E\rangle_{\mathbf{u}_0}$ and $\langle E\rangle_{\mathbf{u}_0}\pm\Delta E$ over a range of times for the case in which $E_N=k_BT$, with $E_D=9E_N$. So as to show the dephasing of the beats we take an unrealistically large damping constant $\gamma_c/(\Delta\omega/2\pi)=0.01$. It should be emphasized that this plot does *not* pertain to an individual experimental run. The plot gives the mean, time-dependent energy together with its rms fluctuation *averaged* over many runs which have the same starting value of the thermal excitation $\mathbf{u}_0$.

V. ANHARMONIC DETECTION OF E_B

The beat signal in the axial-lock voltage due to a C_4 coupling of E_B is estimated by combining the amplitude of the energy excursions [Eq. (4.7)] with the corresponding perturbation to the axial motion [Eq. (3.4)] and has a peak-to-peak value of

$$\frac{\Delta\omega_z(C_4,E_B)}{\omega_z}=2\beta\alpha^2k_BT_c\sqrt{D}\geq R_z\ . \tag{5.1}$$

Here we have redefined the off-resonant driven energy of the cyclotron motion in terms of the temperature of the thermal drive using $E_D=Dk_BT_c$, where D is a dimensionless constant that scales with the strength of the off-resonant drive. As before, this signal must be greater than the axial resolution ($R_z\approx 10^{-8}$) to be observable.

To calculate the inherent systematic in this technique of measuring ω_c' we substitute the time average of E_c into Eq. (3.10) because the C_4 induced shift in the cyclotron frequency is linear in the energy of the trapped ion. E_B therefore averages to zero in Eq. (4.4) giving an estimate for the systematic of

$$\frac{\Delta\omega_c'(C_4,E_B)}{\omega_c'} = -\frac{\beta\alpha^2}{4}[\alpha^2 k_B T_c(1+D)+E_z] \ . \quad (5.2)$$

Using Eq. (5.1), we rewrite this in terms of the amplitude of an observable beat signal ($\approx R_z$),

$$\frac{\Delta\omega_c'(C_4,E_B)}{\omega_c'} \geq \frac{R_z}{8}\left[\alpha^2\frac{(1+D)}{\sqrt{D}}+\frac{E_z}{k_B T_c\sqrt{D}}\right] \geq \frac{\alpha^2 R_z}{4} \ . \quad (5.3)$$

The second inequality, the minimum of this systematic, is obtained when the perturbation due to the cyclotron energy dominates $[\alpha^2 k_B T_c(1+D) > E_z]$ and when the off-resonant drive is adjusted in this limit to give $D=1$. Under these conditions the systematic again scales as $\alpha^2 R_z$ and can be reduced by reducing α or improving the resolution in the axial lock by the methods discussed earlier. The values of $R_z \approx 10^{-8}$ and $\alpha \approx 0.2$ limit our current accuracies to no better than 0.1 ppb which is about an order of magnitude worse than the resolution of 0.01 ppb already demonstrated in Fig. 7. It should be noted that for protons, with the same axial frequency but three times the cyclotron frequency, this systematic limit becomes 0.01 ppb.

Two parameters must be controlled to realize this minimum systematic. Again we must validate the assumption that the cyclotron energy dominates in Eq. (5.2). With our typical value of $\alpha=0.2$ and a 4-K axial temperature, setting D equal to its optimum value of 1 determines the minimum temperature of the heat reservoir coupled to the cyclotron motion. We find that

$$T_c > \frac{T_z}{2\alpha^2} \approx 50 \text{ K} \ . \quad (5.4)$$

Finally, this cyclotron temperature sets [via Eq. (5.1)] a specific value of

$$\beta \approx \frac{R_z}{k_B T_z} \approx 3\times 10^{-5} \text{ (eV)}^{-1} \quad (5.5)$$

that is necessary for minimal detection of the beat signal in the axial lock. If T_c is increased, β must be reduced accordingly to maintain the minimal systematic shown in Eq. (5.3).

Experimentally setting D, β, and T_c to specific values is not easy, thus making it difficult to reach this minimum systematic. Unfortunately, this idealized case was not realized in the beats shown in Fig. 7 primarily because the cyclotron motion was coupled to a 4-K thermal bath rather than this minimum 50-K thermal drive. A good estimate of the systematic in this case can only be calculated if β is known, thereby determining D via Eq. (5.1). For this demonstration we deliberately increased β to $\approx 10^{-4}$ eV^{-1} and the peak-to-peak signal in Fig. 7 is about $3\times R_z$, which puts the C_4 induced systematic at $\approx 2\times 10^{-9}$.

One solution to the systematics associated with anharmonic detection is to take advantage of the fact that they are linear in β. The straight forward way to do this is to alternately take data with $+\beta$ and then $-\beta$. The average of these two measurements would only have a residual systematic associated with the inability to make symmetric changes in β around $\beta=0$ and to maintain equal average energies in the two measurements. A more sophisticated approach would be to modulate β about zero (i.e., modulate the guard voltage about null), thereby symmetrizing the systematics by moving them into FM sidebands leaving an unshifted carrier. In addition, the signal will now modulate coherently with the guard modulation, and we should be able to see a smaller signal by the use of phase-sensitive detection, possibly via the scheme shown in Fig. 9.

The systematics left in this unshifted carrier will then reflect the level to which β can be nulled out prior to the symmetric modulation. As stated earlier we estimate that our guard nulls typically reduce β to less than 4×10^{-6} (eV)$^{-1}$. Combining this with $\alpha=0.2$, $E_z=3\times 10^{-4}$ eV and using Eq. (3.10) gives an uncertainty in this measure of the cyclotron frequency due to the

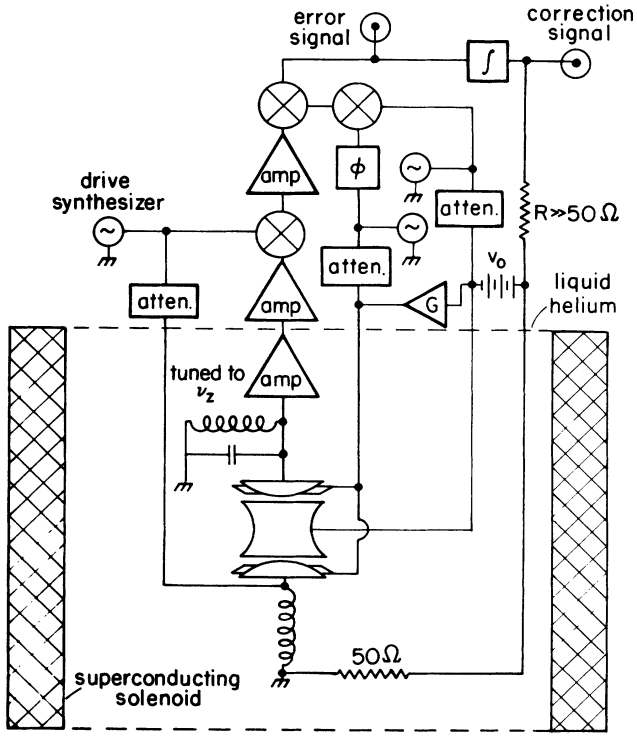

FIG. 9. A schematic representation of a possible experiment using anharmonic detection and a modulation of C_4 about zero. The guard voltage, and therefore β, is modulated. This produces sidebands on the axial motion whose modulation index is sensitive to E_C via Eq. (3.4). The axial-detection scheme is then virtually identical to that currently used (see Fig. 2) except that the drive will now be shifted to this new sideband, adding a slight complication in the mix back to dc. The dispersion quadrature is again used to lock the axial frequency while the amplitude quadrature is monitored to observe changes in the modulation index (and therefore the effective drive strengths) due to changes in the cyclotron energy (beats). In principle, we can reduce the modulation of β while increasing the strength of the axial drive to maintain signal levels until perturbations due to pondermotive forces come into play.

C_4 perturbation of about 0.01 ppb, which is comparable to the current resolution shown in Fig. 7.

It is worth noting that the phase of the beat signal, shown in Fig. 7, is an indication of whether the off-resonant drive is adding energy to the cyclotron motion or conversely taking energy out of the cyclotron motion. One should then be able to use this information in a feedback scheme to continuously cool the cyclotron motion, or by turning the off-resonant drive off at the right phase of the beat signal, one could prepare the cyclotron motion in a cold state. It should also be emphasized that the phase of this beat signal is a reasonably accurate representation of the phase relationship between the drive (which has a clean phase) and the actual cyclotron motion. We therefore have a phase-coherent monitor of the cyclotron motion without the use of a preamplifier at the cyclotron frequency. This may be useful for monitoring the cyclotron motion of the electron in a 6-T magnetic field where building a sensitive preamplifier at 160 GHz is extremely difficult.

VI. CONCLUSION

With these anharmonic-detection schemes we have both simplified the technical aspects and improved the resolution of our mass spectrometer. In this article we have described two methods of monitoring the cyclotron frequency via the axial motion using a fourth-order electrostatic perturbation (proportional to the parameter β and controlled by the potential placed on the guard electrodes). The first method monitors energy absorbed from an rf drive, swept through ω_c', and has a resolution of 10^{-10} with an inherent systematic of 2×10^{-10}. This systematic is fixed for a wide range of values of β for which both the signal and the systematic are proportional to the product $\beta\Delta E_c$. The systematic, under these conditions, can therefore be expressed in terms of the axial resolution and the primary trapping fields and is $\alpha^2 R_z/2$. The second method continuously monitors a beat in the cyclotron energy as the cyclotron motion, in equilibrium with a thermal drive, responds to an off-resonant coherent drive. This method has a resolution of better than 10^{-11} but the inherent systematic limit of 10^{-10} can only be reached by carefully setting the strength of the off-resonant drive D, the value of the fourth-order term β, and the temperature of the thermal drive T_c to specific values. Under these ideal conditions the inherent systematic can also be expressed in terms of the axial resolution and the primary trapping fields and is $\alpha^2 R_z/4$. The value of α can be reduced by making the trap larger or by reducing the trap potential (V_0) thereby reducing ω_z. Also, we might improve the axial resolution R_z by using a Josephson voltage standard for the trap potential. It should therefore be straightforward to reduce this inherent systematic to below 10^{-11}.

We have also pointed out that the inherent systematics associated with this anharmonic detection can be eliminated by modulating β around zero (i.e., modulating the guard voltage around the guard null). We are then limited, as with any other approach in a Penning trap, by our ability to set $\beta=0$. The anharmonic systematic under these conditions would be reduced to 10^{-11} or below 10^{-12} for a modest reduction in α. Modulating β, however, complicates the detection of E_c through the axial motion and necessitates changes in the axial-detection electronics, possibly following the schematic shown in Fig. 9.

In our quest to push the limits of resolution in our cyclotron measurements we have developed a second scheme which has been referred to as "beating the noise." In addition to being able to obtain resonant information through the use of a white noise source, this technique also offers the advantages that come with a continuous, phase-coherent, real-time monitor of the resonant frequency, and as indicated in Eq. (4.11), the monitored beat can be relatively noise free. We hope that the thorough description given of the basic physics that produces the energy beat can be used to make this powerful technique accessible to a wider range of experiments.

ACKNOWLEDGMENTS

We would like to thank Howard Shugart for constructive input during his sabbatical stay at the University of Washington and John Bollinger, Mark Raizen, and Carl Weimer for their comments on the manuscript. The work of F.L.M., D.L.F., P.B.S., and R.S.V. was supported in part by the National Science Foundation under the Mono-Ion Research Grant No. PHY87-05397. The work of S.J. and L.S.B. was supported in part by the Department of Energy Contract No. DE-AS06-88ER-40423.

APPENDIX

In the absence of an external drive, the velocity $\mathbf{u}(t)$ of the cyclotron orbit in a Penning trap obeys the equation of motion

$$\left[\frac{d}{dt}+\frac{1}{2}\gamma_c\right]\mathbf{u}(t)+\omega_c'\hat{\mathbf{z}}\times\mathbf{u}(t)=\mathbf{f}(t)\ . \tag{A1}$$

This motion is coupled (by effective image charges in the conducting trap surfaces) to an external environment which acts as a heat bath at temperature T. The driving force $\mathbf{f}(t)$ in Eq. (A1) accounts for this interaction; it is a random, white noise force. The same coupling gives rise to the damping described by the constant γ_c. In this Appendix we shall solve the equation of motion (A1) to derive the probability distributions used in the text.

The solution can be obtained with the aid of the retarded, tensor Green's function $G_{kl}(t-t')$ defined by

$$\left[\left[\frac{d}{dt}+\frac{1}{2}\gamma_c\right]\delta_{km}-\omega_c'\epsilon_{km}\right]G_{ml}(t-t')=\delta_{kl}\delta(t-t')\ , \tag{A2}$$

where $\delta_{11}=\delta_{22}=1$, $\delta_{12}=0$, $\epsilon_{12}=-\epsilon_{21}=1$, $\epsilon_{11}=\epsilon_{22}=0$, and a summation over repeated indices is implied. The motion is given in terms of this Green's function by

$$u_k(t)=\int_{-\infty}^{t}dt'G_{kl}(t-t')f_l(t')\ . \tag{A3}$$

The tensor Green's function $G_{kl}(t-t')$ may be reduced to a scalar function $\mathcal{G}(t-t')$ by writing

$$G_{kl}(t-t')=\left[\left[\frac{d}{dt}+\frac{1}{2}\gamma_c\right]\delta_{kl}+\omega_c'\epsilon_{kl}\right]\mathcal{G}(t-t') . \tag{A4}$$

Inserting Eq. (A4) into Eq. (A2) yields

$$\left[\frac{d^2}{dt^2}+\gamma_c\frac{d}{dt}+\omega_c'^2\right]\mathcal{G}(t-t')=\delta(t-t') , \tag{A5}$$

where we have neglected terms of order γ_c^2 relative to $\omega_c'^2$, as we shall always do. It is straightforward to establish that

$$\mathcal{G}(t-t')=\frac{\Theta(t-t')}{\omega_c'}e^{-\gamma_c(t-t')/2}\sin\omega_c'(t-t') , \tag{A6}$$

where $\Theta(t-t')$ is the usual unit step function.

We first apply this formulation to compute the thermal averaged velocity correlation function

$$\langle u_k(t)u_l(t')\rangle=\int dt_1dt_2G_{km}(t-t_1)\times G_{ln}(t'-t_2)\langle f_m(t_1)f_n(t_2)\rangle . \tag{A7}$$

The thermal average of the fluctuating forces is given by

$$\langle f_m(t_1)f_n(t_2)\rangle=\frac{\gamma_c k_BT}{2m}\delta_{mm}\delta(t_1-t_2) . \tag{A8}$$

The appearance of the $\delta(t_1-t_2)$ corresponds to a uniform distribution of frequencies—white noise. The overall factor of $\gamma_c k_BT/2m$ is required, as we shall see, to give the proper thermal average $m\langle\mathbf{u}(t)^2\rangle/2=k_BT$. After some calculation using the results above, one finds that

$$\langle u_k(t)u_l(t')\rangle=N_{kl}=\delta_{kl}C(t-t')+\epsilon_{kl}S(t-t') , \tag{A9}$$

where

$$C(t-t')=\frac{k_BT}{m}e^{-\gamma_c|t-t'|/2}\cos\omega_c'(t-t') , \tag{A10}$$

and

$$S(t-t')=\frac{k_BT}{m}e^{-\gamma_c|t-t'|/2}\sin\omega_c'(t-t') . \tag{A11}$$

Clearly $m\langle\mathbf{u}(t)^2\rangle/2=k_BT$.

Correlation functions of arbitrarily high order are needed to construct the probability densities that we need. They are given by a Gaussian factorization which expresses them by the sum of products of all the possible two-time correlations. This factorization is conveniently expressed by the generating functional relation

$$Z[\phi]=\left\langle\exp\left[i\int dt_1\phi_k(t_1)u_k(t_1)\right]\right\rangle=\exp\left[-\frac{1}{2}\int dt_1dt_2\phi_k(t_1)\langle u_k(t_1)u_l(t_2)\rangle\phi_l(t_2)\right] . \tag{A12}$$

Let us first use the generating functional to construct the probability density of finding the velocity $\mathbf{u}$ at time t,

$$P(\mathbf{u},t)=\langle\delta(\mathbf{u}-\mathbf{u}(t))\rangle . \tag{A13}$$

Writing the δ function in terms of its Fourier transform gives

$$P(\mathbf{u},t)=\int\frac{(d^2\mathbf{k})}{(2\pi)^2}e^{i\mathbf{k}\cdot\mathbf{u}}\langle e^{-i\mathbf{k}\cdot\mathbf{u}(t)}\rangle . \tag{A14}$$

This is just the special case of the generating functional with $\phi_l(t)=-k_l\delta(t-t_1)$, and so

$$P(\mathbf{u},t)=\int\frac{(d^2\mathbf{k})}{(2\pi)^3}e^{i\mathbf{k}\cdot\mathbf{u}}\exp[-\tfrac{1}{2}k_l\langle u_l(t)u_m(t)\rangle k_m] . \tag{A15}$$

Using Eqs. (A9)–(A11), we have

$$P(\mathbf{u},t)=\int\frac{(d^2\mathbf{k})}{(2\pi)^2}e^{i\mathbf{k}\cdot\mathbf{u}}\exp\left[-\frac{k_BT}{2m}\mathbf{k}^2\right]=\frac{m}{2\pi k_BT}\exp(-\tfrac{1}{2}m\mathbf{u}^2/k_BT) , \tag{A16}$$

which is the proper, time-independent Maxwell-Boltzmann distribution.

The probability density

$$P(\mathbf{u},t;\mathbf{u}',t')=\langle\delta(\mathbf{u}-\mathbf{u}(t))\delta(\mathbf{u}'-\mathbf{u}(t'))\rangle \tag{A17}$$

for finding the velocity $\mathbf{u}$ at time t and the velocity $\mathbf{u}'$ at time t' can be calculated in the same way. Again introducing Fourier transforms for the δ functions and using Eqs. (A9)–(A12), we have

$$P(\mathbf{u},t;\mathbf{u}',t')=\int\frac{(d^2\mathbf{k})}{(2\pi)^2}\frac{(d^2\mathbf{k}')}{(2\pi)^2}e^{i(\mathbf{k}\cdot\mathbf{u}+\mathbf{k}'\cdot\mathbf{u}')}\times\exp\left[-\frac{k_BT}{2m}(\mathbf{k}^2+\mathbf{k}'^2)\right]\times\exp[-k_l\langle u_l(t)u_m(t')\rangle k_m'] . \tag{A18}$$

The calculation is facilitated by combining the two 2-vectors $\mathbf{u},\mathbf{u}'$ into a four-component vector $U=(u_1,u_2,u_1',u_2')$ and similarly writing $K=(k_1,k_2,k_1',k_2')$ to achieve the matrix form

$$P(\mathbf{u},t;\mathbf{u}',t')=\int\frac{(d^4k)}{(2\pi)^4}e^{iKU}\exp\left[-\frac{k_BT}{2m}KMK\right] . \tag{A19}$$

Here M is the matrix

$$M=\begin{bmatrix}1 & N\\ N^T & 1\end{bmatrix} \tag{A20}$$

whose entries are 2×2 matrices with

$$N_{kl}=\langle u_k(t)u_l(t')\rangle=e^{-\gamma_c|t-t'|/2}[\delta_{kl}\cos\omega_c'(t-t')+\epsilon_{kl}\sin\omega_c'(t-t')] \tag{A21}$$

and N^T its matrix transpose. The calculation is essentially trivial because

$$NN^T=N^TN=e^{-\gamma_c|t-t'|}1 \ . \tag{A22}$$

Hence

$$M^{-1}=\frac{1}{1-e^{-\gamma_c|t-t'|}}\begin{bmatrix}1 & -N\\ -N^T & 1\end{bmatrix} . \tag{A23}$$

Moreover, since

$$\det\begin{bmatrix}1 & -N\\ -N^T & 1\end{bmatrix}=\det\begin{bmatrix}1 & N\\ N^T & 1\end{bmatrix} , \tag{A24}$$

the determinant of M is easily evaluated from

$$(\det M)^{-1}=\det M^{-1}$$
$$=(1-e^{\gamma_c|t-t'|})^{-4}\det M \ , \tag{A25}$$

which requires that

$$\det M=(1-e^{-\gamma_c|t-t'|})^2 . \tag{A26}$$

We may now use the standard evaluation of the Gaussian integral in Eq. (A19) that is provided by completing the square, namely

$$P(\mathbf{u},t;\mathbf{u}',t')=\left[\frac{m}{2\pi k_BT}\right]^2\det{}^{-1/2}M$$
$$\times\exp\left[-\frac{m}{2k_BT}UM^{-1}U\right] . \tag{A27}$$

Thus, with the aid of Eqs. (A26) and (A23), we have

$$P(\mathbf{u},t;\mathbf{u}',t')=\left[\frac{m}{2\pi k_BT}\right]^2\frac{1}{1-e^{-\gamma_c|t-t'|}}\exp\left[-\frac{m}{2k_BT}\frac{\mathbf{u}^2+\mathbf{u}'^2-2u_kN_{kl}u_l'}{1-e^{-\gamma_c|t-t'|}}\right] . \tag{A28}$$

Since N_{kl} is exponentially damped for large time differences, in the limit $|t-t'|\gg 1/\gamma_c$,

$$P(\mathbf{u},t;\mathbf{u}',t')\simeq\left[\frac{m^2}{2\pi k_BT}\right]^2\exp\left[-\frac{m}{2k_BT}(\mathbf{u}^2+\mathbf{u}'^2)\right]$$
$$\simeq P(\mathbf{u},t)P(\mathbf{u}',t') . \tag{A29}$$

At large times, the joint probability is the uncorrelated product of the probabilities for finding the velocities $\mathbf{u}$ and $\mathbf{u}'$.

Although this probability density is symmetrical in $\mathbf{u},t;\mathbf{u}',t'$, its significance is most clearly brought out by an unsymmetrical treatment. To this end, we note that the matrix $N_{kl}(t-t')$, except for the overall exponential decay factor, is simply the rotation matrix that carries the undamped motion from $\mathbf{u}'(t')$ to $\mathbf{u}'(t)$. That is

$$N_{kl}(t-t')u_l'=e^{-\gamma_c|t-t'|/2}u_k'(t,t') \tag{A30}$$

defines the velocity at time $t,\mathbf{u}'(t,t')$ which is obtained by the free, undamped cyclotron motion starting out with the velocity $\mathbf{u}'$ at time t'. Using this notation, we may write

$$P(\mathbf{u},t;\mathbf{u}',t')=\left[\frac{m}{2\pi k_BT}\right]^2\frac{1}{1-e^{-\gamma_c|t-t'|}}\exp\left[-\frac{m}{2k_BT}\left[\frac{[\mathbf{u}-e^{-\gamma_c|t-t'|/2}\mathbf{u}'(t,t')]^2}{1-e^{-\gamma_c|t-t'|}}+\mathbf{u}'^2\right]\right] . \tag{A31}$$

The conditional probability density for finding the velocity $\mathbf{u}$ at time t given that the velocity at time $t_0=0$ was $\mathbf{u}_0$ is thus given by

$$P_{\mathbf{u}_0}(\mathbf{u},t)=\frac{P(\mathbf{u},t;\mathbf{u}_0,0)}{P(\mathbf{u}_0,0)}$$
$$=\left[\frac{m}{2\pi k_BT}\right]\frac{1}{1-e^{-\gamma_c|t|}}\exp\left[-\frac{m}{2k_BT}\frac{[\mathbf{u}-e^{-\gamma_c|t|/2}\mathbf{u}_0(t)]^2}{1-e^{-\gamma_c|t|}}\right] . \tag{A32}$$

This is the formula (4.12) quoted in the text.

Finally, let us establish the result (4.11) for the line shape

$$\langle|E(\omega)|^2\rangle=\frac{1}{2t_0}\int_{-t_0}^{t_0}dt\,dt'e^{i\omega(t-t')}\langle F(t)F(t')\rangle \ . \tag{A33}$$

The correlation function $\langle F(t)F(t')\rangle$ is a function only of the time difference $\tau=t-t'$, and so we change integration variables to τ and $\bar{t}=(t+t')/2$. The correlation function vanishes for $\tau\gg 1/\gamma_c$, which are times τ that are yet small in comparison with t_0, and so the τ integration may be extended to an infinite range $-\infty<\tau<\infty$. The remaining $\bar{t}$ integration now simply produces a factor of $2t_0$. Thus

$$\langle|E(\omega)|^2\rangle=\int_{-\infty}^{\infty}d\tau\,e^{i\omega\tau}\langle F(\tau)F(0)\rangle \ . \tag{A34}$$

In view of Eq. (4.9),

$$\langle F(\tau)F(0)\rangle = \langle [E_N(\tau)-k_BT][E_N(0)-k_BT]\rangle + \langle E_B(\tau)E_B(0)\rangle \ . \quad \text{(A35)}$$

Since $E_B(\tau)$ is linear in the fluctuating variable $\mathbf{u}(\tau)$ while $E_N(\tau)$ is even in this variable, the cross correlation $\langle E_N(\tau)E_B(0)\rangle$ vanishes. The Gaussian nature of the noise implies that the correlation function of $\mathbf{u}$ factorizes as implied by the generating functional (A12). Hence, since $E_N = m\mathbf{u}^2/2$ with $m\langle \mathbf{u}^2\rangle/2 = k_BT$,

$$\begin{aligned}\langle [E_N(\tau)-k_BT][E_N(0)-k_BT]\rangle &= \tfrac{1}{2}m^2\langle u_k(\tau)u_l(0)\rangle\langle u_h(\tau)u_l(0)\rangle \\ &= \tfrac{1}{2}(k_BT)^2N_{kl}(\tau)N_{kl}(\tau) \ , \\ &= (k_BT)^2e^{-\gamma_c|\tau|} \ . \end{aligned} \quad \text{(A36)}$$

The correlation function of the beating energy is given by

$$\begin{aligned}\langle E_B(\tau)E_B(0)\rangle &= m^2\langle u_k(\tau)u_l(0)\rangle v_k(\tau)v_l(0) \\ &= 2(k_BT)E_De^{-\gamma_c|\tau|/2}\cos(\Delta\omega\tau) \ . \end{aligned} \quad \text{(A37)}$$

Using these results for the correlation functions, the Fourier transform (A33) gives the result (4.11) quoted in the text.

[1] R. S. Van Dyck, Jr., F. L. Moore, D. L. Farnham, and P. B. Schwinberg, Int. J. Mass Spectrom. Ion Proc. **66**, 327 (1985); Bull. Am. Phys. Soc. **31**, 244 (1986).

[2] R. S. Van Dyck, Jr., F. L. Moore, D. L. Farnham, and P. B. Schwinberg, in *Frequency Standards and Metrology,* edited by A. De Marchi (Springer-Verlag, Berlin, 1989), pp. 349–355.

[3] F. L. Moore, D. L. Farnham, P. B. Schwinberg, and R. S. Van Dyck, Jr., Nucl. Instrum. Methods Phys. Res. **B43**, 425 (1989).

[4] E. A. Cornell, Ph.D. thesis, Massachusetts Institute of Technology, 1990; see also E. A. Cornell, R. M. Weisskoff, K. R. Boyce, R. W. Flanagan, Jr., G. P. Lafyatis, and D. E. Pritchard, Phys. Rev. Lett. **63**, 1674 (1989).

[5] Ch. Gerz, D. Wilsdorf, and G. Werth, Z. Phys. D **17**, 117 (1990).

[6] R. S. Van Dyck, Jr., P. B. Schwinberg, and H. G. Dehmelt, in *New Frontiers in High Energy Physics,* edited by B. Kursunoglu, A. Perlmutter, and L. F. Scott (Plenum, New York, 1978), pp. 159–181.

[7] R. S. Van Dyck, Jr., P. B. Schwinberg, and H. G. Dehmelt, Phys. Rev. D **34**, 722 (1986).

[8] T. Kinoshita and W. B. Lindquist, Phys. Rev. D **42**, 636 (1990). See also T. Kinoshita, Metrologia **25**, 233 (1988) and IEEE Trans. Instrum. Meas. **38**, 172 (1989).

[9] R. S. Van Dyck, Jr., P. B. Schwinberg, and H. G. Dehmelt, Phys. Rev. Lett. **47**, 1679 (1981); **59**, 26 (1987).

[10] P. B. Schwinberg, R. S. Van Dyck, Jr., and H. G. Dehmelt, Phys. Lett. **81A**, 119 (1981).

[11] G. Gabrielse, X. Fei, L. A. Orozco, R. L. Tjoelker, J. Hass, H. Kalinowsky, T. A. Trainor, and W. Kells, Phys. Rev. Lett. **65**, 1317 (1990).

[12] F. L. Moore, D. L. Farnham, P. B. Schwinberg, and R. S. Van Dyck, Jr., Phys. Scr. **T22**, 294 (1988).

[13] M. S. Dewey, E. G. Kessler, R. D. Deslattes, and G. L. Green, in *Abstracts of the Twelfth International Conference on Atomic Physics,* edited by W. E. Baylis, G. W. F. Drake, and J. W. McConkey (University of Windsor, Ontario, 1990).

[14] R. S. Van Dyck, Jr., H. A. Schuessler, R. D. Knight, D. Dubin, W. D. Phillips, and G. Lafyatis, Phys. Scr. **T22**, 228 (1988).

[15] R. S. Van Dyck, Jr., D. L. Farnham, and P. B. Schwinberg, J. Mod. Opt. **39**, 243 (1992).

[16] R. S. Van Dyck, Jr., in *Quantum Electrodynamics,* Advanced Series on Directions in High Energy Physics, edited by T. Kinoshita (World Scientific, Singapore, 1990), Vol. 7, pp. 322–388.

[17] L. S. Brown and G. Gabrielse, Rev. Mod. Phys. **58**, 233 (1986).

[18] P. B. Schwinberg, F. L. Moore, D. L. Farnham, and R. S. Van Dyck, Jr., Bull. Am. Phys. Soc. **31**, 244 (1986); see also R. S. Van Dyck, Jr., F. L. Moore, D. L. Farnham, and P. B. Schwinberg, Rev. Sci. Instrum. **57**, 593 (1986).

[19] L. S. Brown and G. Gabrielse, Phys. Rev. A **25**, 2423 (1982).

[20] R. S. Van Dyck, Jr. and P. B. Schwinberg, in *Precision Measurement and Fundamental Constants II,* edited by B. N. Taylor and W. D. Phillips, Natl. Bur. Stand. (U.S.) Spec. Publ. No. 617 (U.S. GPO, Washington, DC, 1984), pp. 349–352; Phys. Rev. Lett. **47**, 395 (1981).

[21] D. J. Wineland, W. M. Itano, and R. S. Van Dyck, Jr., Adv. At. Mol. Phys. **19**, 135 (1983).

[22] H. Dehmelt, in *Atomic Physics,* edited by D. Kleppner and F. Pipkin (Plenum, New York, 1981), Vol. 7, pp. 337–372.

[23] R. S. Van Dyck, Jr., D. J. Wineland, P. A. Ekstrom, and H. G. Dehmelt, Appl. Phys. Lett. **28**, 446 (1976).

[24] G. Gabrielse and F. C. Mackintosh, Int. J. Mass Spectrom. Ion Proc. **57**, 1 (1984); see also E. C. Beaty, J. Appl. Phys. **61**, 2118 (1987); G. Gabrielse, L. Haarsma, and S. L. Rolston, Int. J. Mass Spectrom. Ion Proc. **88**, 319 (1989).

[25] G. Gabrielse, Phys. Rev. A **27**, 2277 (1983).

[26] Press Release OXFORD, Oxford Instruments Limited, Eynsham, Oxford, OX8 1TL.

[27] J. B. Camp, T. W. Darling, and R. E. Brown, J. Appl. Phys. **69**, 7126 (1991).

[28] R. S. Van Dyck, Jr., F. I. Moore, D. L. Farnham, and P. B. Schwinberg, Bull. Am. Phys. Soc. **31**, 973 (1986).

[29] R. M. Weisskoff, G P. Lafyatis, K. R. Boyce, E. A. Cornell, R. W. Flanagan, Jr., and D. E. Pritchard, J. Appl. Phys. **63**, 4599 (1988); see also R. M. Weisskoff, Ph.D. thesis, M.I.T., 1988 (unpublished).

[30] F. L. Lloyd, C. A. Hamilton, J. A. Beall, D. Go, R. H. Ono, and R. E. Harris, IEEE Electron Device Lett. **EDL-8**, 449 (1987); see also C. A. Hamilton, F. L. Lloyd, C. Kao, and W. C. Goeke, IEEE Trans. Instrum. Meas. **38**, 314 (1989).

[31] P. B. Schwinberg and R. S. Van Dyck, Jr., Bull. Am. Phys. Soc. **23**, 40 (1978).

[32] G. Gabrielse and H. G. Dehmelt (unpublished).